Deliverable D9.5

Deliverable Title:	Hyperspectral mapping pipeline/guideline
Due date of deliverable:	15 December 2021
Nature[1]:	R
Dissemination level[2]:	P
Work package:	9
Lead beneficiary:	JacobsUni
Contributing beneficiaries:	INAF
Document status:	Final

Start date of project:	01 February 2020
Project Duration:	48 months
Co-ordinator:	Prof Nigel Mason

Executive Summary / Abstract:

The main multispectral and hyperspectral datasets relevant to planetary geologic mapping are introduced, as well as their use for reflectance studies, analysis and mapping. Examples of datasets and their spectral characteristics are described for the case of the Moon, Mercury, Mars and Vesta, in each case including general spectral properties and dataset-specific relevant information. High-level and derived products specifically useful for geologic mapping products are introduced. Finally, access to datasets, tools and supporting literature is included in the document.

Table of Contents

List of Acronyms

Acronym	*Description*
BDI	Band Depth I
BDII	Band Depth II
CAT	CRISM Analysis Toolkit
CRISM	Compact Reconnaissance Imaging Spectrometer for Mars
DDR	Derived Data Record
DEM	Digital Elevation Model
DLR	Deutsches Zentrum für Luft- und Raumfahrt
DTM	Digital terrain model
EDR	Experiment Data Record
ENVI	Environment for Visualizing Images
EPN	EuroPlanet
ESA	European Space Agency
GIS	Geographic Information System
HED	Howardites, Eucrites, Diogenites achondritic meteorites
IDL	Interactive Data Language
ISIS	Integrated Software for Imagers and Spectrometers
JCAT	Java CRISM Analysis Tool
LRM	Low Reflectance Materials
M^3	Moon Mineralogy Mapper
MarsSI	Mars System of Information
MASCS	Mercury Atmospheric and Surface Composition Spectrometer
MDIS	Mercury Dual Imaging System
MESSENGER	Mercury Surface, Space Environment, Geochemistry and Ranging
MeX	Mars Express
MICA	Minerals Identified through CRISM Analysis

MidIR	Middle Infrared
ML	Machine Learning
MRO	Mars Reconnaissance orbiter
MTRDR	Map-projected Targeted Reduced Data Record
NASA	National Aeronautics and Space Administration
NIR	Near-infrared
npFe°	Nano phase iron particle
OAT	OMEGA Analysis Tool
ODE	Orbital Data Explorer
OMEGA	Observatoire pour la Minéralogie, l'Eau, les Glaces et l'Activité
PDS	Planetary Data System
PSA	Planetary Science Archive
PSUP	Planetary SUrface Portal
RGB	Red, Green, Blue (colour maps)
SWIR	short wavelength infrared
TER	Targeted Empirical Record
TES	Thermal Emission Spectrometer
THEMIS	Thermal Emission Imaging System
TRDR	Targeted Reduced Data Record
UVVS	Ultraviolet and Visible Spectrometer
VESPA	Virtual Observatory in Planetary Science
VIRS	Visible InfraRed mapping Spectrometer
VNIR	Visible to near-infrared
WAC	Wide Angled Camera
WP	Work Package

1. Introduction on Hyper- Multispectral dataset

a) Hyperspectral and Multispectral datasets

Multi- and hyperspectral remote sensing experiments over various Solar System bodies allow to infer mineralogical compositions of surface materials. Almost all planetary bodies in the inner Solar System, some minor bodies, as well as the surface of some moons in Jupiter and Saturn systems have been mapped with such techniques providing a wide range of data.

Spectral data are acquired with imaging instruments that in some cases achieve spatial resolutions comparable with that of panchromatic imagers, allowing mappers to analyse with great detail the local and global compositional variations, as well as to detect specific spectrally dominating mineralogical phases.

Depending on the target planetary body, the data volume available and other aspects (e.g. spatial vs. spectral resolution) the various instruments can acquire spectral data in two different modes (e.g. Bishop et al. 2019):

a) hyperspectral data: a data set with a high number of spectral channels in a specific wavelength range;
b) multispectral data: few spectral channels, often associated with colour filters, in a specific wavelength range.

Each type of mineral has unique spectral characteristics which allow it to be distinguished from other minerals in the form of absorptions of high reflectance in specific wavelengths/ spectral ranges. Considering the various types of absorptions, different spectral ranges can be investigated to identify the minerals present on a surface. For example, M-O spin forbidden transition (e.g. due to iron in pyroxene or olivine) and interval charge transfer absorption can be investigated ranging from the ultraviolet to the visible spectrum (e.g. Burns 1993). Charge transfer and crystal field absorption (e.g. Burns 1993, Clark 1999) as well as some overtones related to hydration (e.g. M-OH, H-O-H) or carbonates (due to $(CO_3)^{2-}$ anion) (e.g. Farmer 1974, Clark 1999) can be investigated in the VNIR range, which usually refers to short-wave infrared (up to 2.5 μm). Extending to the NIR range, which is up to 5/6 μm, other important absorptions (tones or overtones) can be recognized. These are attributable to molecular processes of water (presence of hydrated minerals or ice on the surface), carbonates or other phases (e.g. Farmer 1974, Clark 1999). In the MidIR (up to about 15 μm) molecular absorptions (i.e. vibrational), often fundamental, are present (e.g. Farmer 1974). However, emittance is investigated with this spectral range rather than reflectance, and up to date these observations have been performed only for Mars (TES, Christensen et al. 1992, THEMIS, Christensen et al. 2004) and the Moon (DIVINER, Page et al. 2010).

In this document we focus on spectral data in the VNIR range for the following reasons: i) the datasets described are relative to the reflectance of the surfaces; ii) we have coverage of several planetary bodies in this range; iii) it is the most used range for spectral analysis and mapping of minerals on planetary surfaces.

b) VNIR reflectance spectra

The spectral information acquired in the VNIR indicates the properties of the materials reflecting the solar radiance. In the last decades several bodies have been investigated by a hyperspectral imaging system, although for Mercury and Moon multispectral cameras have also provided datasets of high scientific relevance. To this date, no hyperspectral imaging data have been acquired on Mercury. MESSENGER mission had a hyperspectral punctual instrument (MASCS, McClintock and Lankton, 2007) and a colour camera, MDIS (Hawkins et al., 2007), that globally imaged its surface.

Conversely, openly available reflectance data covering the Moon exist: global usable hyperspectral data from M^3 (Pieters et al., 2009) are available, but no global higher level products have been released by the M^3 team so far. Therefore the commonly used higher level products suitable to characterise the lunar surface consists of Clementine multispectral data (e.g. McEwen and Robinson, 1997).
In general, planetary orbital experiments can acquire spectra ranging from visible up to 3 μm, e.g. (M^3, Chandraayan-1 mission, Pieters et al., 2009); up to 4 μm, e.g. (CRISM, MRO, Murchie et al., 2007); or up to 5 μm, e.g. (OMEGA, MeX, Bibring et al., 2004; VIRS, Dawn, De Sanctis et al., 2011). In general, data are corrected based on observation geometry in order bring them to similar comparable and consistent conditions (e.g. illumination at 30° and emission at 0°). Some planetary bodies can even benefit from the support of detailed topographic information, or even a DTM, to photometrically correct as best as possible the reflectance properties with respect to physical and morphological variations of the surface.
The VNIR spectral range, as briefly reported above, allows the distinction of several minerals, which are attributable to rock-forming minerals as well as secondary phases. In particular, some silicates, sulfates and carbonates can be distinguished. Moreover, VNIR range allows to differentiate regions that are brighter than others (e.g. due to higher abundance of brighter, sometimes featureless, minerals, or different particle sizes, or different roughness variation of the surface). Finally, by taking into account relative variation in spectral information it is possible to highlight fresher regions and differentiate them with respect to more mature areas where the space weathering strongly affected the reflectance signature (e.g. Domingue et al. 2014).

c) Spectral Analysis and Mapping

Reflectance spectral images can be used to differentiate regions of the surface of a body with differences in mineral composition, which often is directly correlated with differences in elemental composition or formation processes of surface materials. These images can also give indications on some physical properties of the surfaces (e.g. particle size or roughness) provided that the composition of surface materials is defined. Moreover, it is possible to have some indirect information related to abundance of bright or dark featureless minerals, and to the presence of some phases

that are in general affecting the spectral slope, e.g. oxidized phases on Mars or nano phase iron particle, npFe°, on the Moon.
This type of information can be retrieved quantitatively or qualitatively following different analytical methodologies. Here we recall some preliminary, and most common, ways to analyse a large dataset aiming at highlighting or detecting different mineral phases, as well as comparing regions with different spectral properties.
In fact, almost all the datasets can be analysed by defining appropriate spectral indices, considering wavelengths that can help to identify and compare the different minerals present on the surface. In general, it is possible to identify a mineral highlighting a specific absorption band. Moreover, an absorption peak shift can be calculated considering the position of the band centre of a specific absorption. In addition we can consider the band depth of a specific absorption, which can be calculated around (or exactly at) the band centre. Slopes (i.e. band ratios) can also give important information related to some absorptions or to significant variation of the spectral signature. In some cases also comparing band areas or using the ratio between the band areas of two absorptions allows to understand the relations or differences among two close absorptions. We will give some general indication on how these parameters can be calculated in section 3 with more details on the Moon, Mars, Mercury and Vesta in 3.1, 3.2, 3.3 and 3.4, respectively. All the generated spectral parameters (ratios, band depth, band areas etc.) can finally be plotted in a map, locally or globally, to emphasize mineralogical variations. Section 4 describes high-level data products released by specific instrument teams, where to retrieve them, and how to use the data for integration and comparison with morphological and stratigraphic observations (see also PLANMAP deliverables[1] for further details on spectral data and data integration).
Moreover, RGB combinations/maps can often be important to show the presence of specific mineral phases or to compare information for different mineral phases by combining three different spectral indices related to those phases.

Specific parameters such as the reflectance at a certain wavelength or principal components (Richards et al., 1999) can also be used in a RGB map to emphasize certain characteristics. In section 4 we will provide some information about RGB maps and where to download some of them.

2. Examples of VNIR main spectral properties and datasets

In this section we will briefly give some information on the VNIR spectral properties of the surfaces of some planetary bodies and on the datasets, calibrated to reflectance, that can be used. We put particular emphasis on the availability of multi- or

[1] https://wiki.planmap.eu/display/public/Deliverables

hyperspectral data, and we indicate where they can be downloaded and used to support spectral analyses.

2.1 The Moon

2.1.1 Main spectral properties of the Lunar surface

Moon spectra are mainly characterized by two absorption bands at 1 µm and 2 µm. These bands are caused by absorption of photons, primarily by Fe^{2+}. The exact band position and shape are determined by the relative proportion of Fe^{2+}, Ca^{2+} and Mg^{2+} in the M1 and M2 sites of the pyroxene and olivine crystal structures, or in glass material (Burns, 1993). Other iron bearing minerals can have absorption associated to Fe^{2+} in similar spectral regions but they are not relevant for the Moon, with a possible exception for spinels (e.g. Chromite).

Furthermore, Lunar spectra have a strong spectral reddening due to the presence of $npFe^0$ caused by space weathering effects.

Some features related to potential water (hydration) or ice presence have been considered close to the 3 µm wavelength in M^3 data (e.g. Pieters et al. 2009).

2.1.2 Data sets

The most comprehensive hyperspectral dataset available for the Moon has been acquired by the **Moon Mineralogical Mapper** (Pieters et al., 2009) onboard Chandrayaan-1 mission which operated between 2008 and 2009.

M^3 is an imaging pushbroom spectrometer, covering the 446-3000 nm spectral range. M^3 acquired data at two different spatial resolutions: 140 m/px for the global coverage, with a spectral sampling of 20 or 40 nm, and 70 m/px for specific targets, w specific targets, with a spectral sampling of 10 nm (https://pds-geosciences.wustl.edu/workshops/M3_workshop_Dec10.htm).

The M^3 data are available in different levels of processing: raw data (Level 0), radiance data (Level 1b) and reflectance data (photometrically corrected) (Level 2). In addition, the M^3 team released the backplains file, containing information such as latitude, longitude and illumination condition geometries. All data are available in the PDS node (https://pds- imaging.jpl.nasa.gov/volumes/m3.html) and in the Lunar Data Orbiter Explorer (https://ode.rsl.wustl.edu/moon/).

Reflectance data, calibrated and photometrically corrected are analysis-ready.

There are no specific tools for spectral analysis. Therefore, to calculate specific spectral indices, it is necessary the use of appropriate programming languages (e.g. IDL, Python, MatLAB), which allows writing ad hoc programs. ENVI or GIS software packages can be helpful for visualization and some specific operations and classifications.

2.2 Mars

2.2.1 Main spectral properties of the Martian surface

The most visible feature on Mars is a red dust made of ferric oxides that almost covers the surface entirely. The brightest regions are also the dustier ones. Ferric phases are recognizable through an absorption edge at 0.53 µm caused by several Fe^{3+} transitions, and also exhibit a broad feature between 0.75 and 1 µm (e.g. Poulet et al 2007, Pelkley et al. 2007, Viviano-Beck et al. 2014). At the remaining wavelengths the spectrum is relatively featureless. Where the dust layer is not too thick, it is possible to probe the surface composition, and to reveal its mineralogical heterogeneity. Dark regions are relatively dust free and the crust is directly exposed. Mars has a primary igneous upper crust, with plagioclase and pyroxenes as the most abundant components. Olivine is also an important rock-forming mineral usually found where material was excavated from depth, such as on the rim of large impact basins such as Argyre, Hellas and Isidis. These mineral phases can show absorption attributable mainly to Fe^{2+} crystal field transitions of iron (Burns, 1993). Moreover, several hydrated mineral phases, silicates or sulfates, as well as carbonates can be detected on Mars. These are evidenced by narrower absorption features, attributable to molecular absorption overtones, usually around 1.9 µm (sometimes also 1.4 µm), and in the range between 2.1 and 2.6 µm (e.g. Clark 1990). Some features can also be found in the range between 3 and 5 µm, although this range on Mars is often saturated by water absorption.

2.2.2 Data sets

Among the data available for Mars, we present here the two most used datasets for mineralogical analysis: OMEGA and CRISM data. OMEGA is an instrument designed for global analysis, while CRISM is mostly dedicated to small-scale analysis.

The OMEGA instrument, onboard ESA's Mars Express spacecraft, is made of two co-aligned grating spectrometers, one operating in the VNIR in the range 0.38-1.05 µm, the other in the SWIR in the range 0.93-5.1 µm, with 352 spectral channels. The spatial resolution of the instrument varies from 0.3 to 4.8 km/pixel (depending on altitude), while the spectral resolution varies from 7 to 20 nm. OMEGA's signal-to-noise ratio allows the detection of absorption bands as shallow as ~1 % (Bibring et al., 2004).

OMEGA provides a global coverage at 2-5 km spatial resolution and high-resolution (<350 m) spectral images of selected areas (Bibring et al., 2004).

The primary source for OMEGA data is the ESA PSA. Through a cooperative agreement between ESA and NASA, the PDS Geosciences Node is hosting a copy of the OMEGA data archive (https://pds-geosciences.wustl.edu/missions/mars_express/omega.htm).

Online tools:

- Mars ODE - provides search, display, and download tools for OMEGA data set
- OMEGA Analysis Tool (OAT) - a collection of ENVI and IDL procedures for reading, displaying, and analyzing OMEGA data using SOFT10 code as a basis (for Windows).

-MarsSI (Mars System of Information, https://emars.univ-lyon1.fr/MarsSI/), a web GIS application. The MarsSI facility is part of the web portal PSUP (Planetary SUrface Portal) developed by the Observatories of Paris Sud and Lyon. Footprints of OMEGA data can be visualized in MarsSI by activating the "MEX–OMEGA" layer and data can be downloaded as EDR (raw) Level-1B (Quantin-Nataf et al., 2018). The calibrated OMEGA data (Level-2) can be accessed via the PSUP portal (Poulet et al., 2018).

CRISM is a visible-infrared hyperspectral imager which operates in the wavelength range 362-3920 nm. The spectral properties of the surface can be collected through two different observation modes, depending on the spatial and spectral resolution needed:

- In the "targeted mode", data are acquired at full spatial and spectral resolution, sampling 544 wavelengths and with a spatial resolution of 15-19 m/pixel, depending on the altitude.
- The "multispectral survey mode" acquires data with a spatial resolution of 100-200 m/pixel and sampling 72 of the 544 wavelengths available.

Each pixel which composes the image has its own spectrum. For more technical information on the instrument see Murchie et al. (2007).

CRISM targeted observations are of particular significance as they allow a detailed study of the mineralogical characteristics of small-scale deposits, previously only accessible by in situ investigations with rovers. This type of data is available in NASA archive ODE/PDS.

There are various CRISM products which can be downloaded. More information about the various products can be found here:
https://ode.rsl.wustl.edu/mars/pagehelp/Content/Missions_Instruments/Mars%20Reconnaissance%20Orbiter/CRISM/CRISM%20Product%20Primer/CRISM%20Product%20Primer.htm

In order to process a CRISM targeted observation the following products are needed:

- I/F TRDR: these are radiometrically calibrated CRISM spectra. I/F is defined as the spectral radiance divided by the solar spectral irradiance of the Sun at Mars distance divided by pi.
- DDR: these products include the geometric information (latitude, longitude, incidence, emission, and phase angles) needed to map project the I/F products, and information on surface physical properties, which is necessary to correct the I/F TRDRs for photometric, atmospheric, and thermal effects.

To download these files from ODE/PDS, one should choose CRISM MTRDR or TER from the menu on the left in the map display page. The data will now appear on the map, here you can select the footprints of interest and click on the yellow box which appears in the upper right corner of the map to see the selection result list. From here you can click on the file names and a new window will open. DDRs and TRDRs are under the "related products" label. These products have an .IMG extension and should be downloaded with their label file (.LBL), which contains all the necessary information on the observation. Additionally, the data is usually divided into two parts, one for the

visible-near infrared part of the spectrum (0.362-1 µm) and one for the infrared (1-3.92 µm). According to the established nomenclature both TRDRs and DDRs have a S in the file name if the data is in the visible-near infrared range and a L if it refers to the infrared.

Tools:

-The CAT allows users to read, display and analyze CRISM data. It can be freely downloaded here: https://pds-geosciences.wustl.edu/missions/mro/crism.htm, although a licensed ENVI+IDL installation is required. In order to proceed with the analysis, as a first step, original PDS files need to be converted to CAT format. We can then correct the I/F TRDR data for atmospheric absorption (volcano scan method, McGuire et al. 2009) and photometric effect. Note that atmospheric correction is only necessary for infrared data.
More information on these procedures can be found here:

- Introduction to CAT
  https://pds-geosciences.wustl.edu/missions/mro/CRISM_Workshop_090322_CAT_MFM.pdf
- CAT user's guide
  https://pds-geosciences.wustl.edu/missions/mro/cat_user_guide.pdf

-Alternatively, a Java-based tool for analyzing CRISM data cubes (JCAT), which does not require ENVI, has been recently developed by the CRISM team. For more information see http://crism.jhuapl.edu/JCAT/ and the tutorial here
http://crism.jhuapl.edu/JCAT/JCAT_Tutorial.pdf

2.3 Mercury

2.3.1 Main spectral properties of the surface of Mercury

Differently from Moon and Mars, Mercury does not reveal up to now strong spectral features, but mainly variation in slope and reflectance, which seems to correlate with specific features. So red/orange terrains relatively bright correspond with Faculae/Pyroclastic deposits. Hollows look like to have peculiar colour within specific RGB and a high reflectance with bluer slope. Whereas specific terrains are dark with red or blue slopes. Some of them are possibly attributable to the presence of graphite whereas others could be attributable to space weathering or other unclear aspects. A summary can be found in Rothery et al. (2020 reference therein) and more details are reported in the next section.

2.3.2 Data sets

Mercury surface multispectral coverage between 430 and 1000 nm, has been provided by **MESSENGER/MDIS-WAC** in 11 spectral bands. The dataset, which

includes raw and calibrated data, is publicly available at the Mercury ODE (https://ode.rsl.wustl.edu/mercury/).
Mercury global coverage is available for 8 of the 11 filters: F (430.0 nm), C (480.4 nm), D, (559.2 nm), E (628.8 nm), G (749.0 nm), L (828.6 nm), J (898.1 nm), I (996.8 nm) (Hawkins et al., 2007).
The product necessary for performing a large and local scale spectral analysis, is the MDIS-WAC 8-color mosaic. The messenger team provided a number of high level products, including the 8-color global mosaic at 665 m/px (https://astrogeology.usgs.gov/search/map/Mercury/Messenger/Global/Mercury_MESSENGER_MDIS_ClrMosaic_global_665m_v3?p=1&pb=1#downloads).

If the user needs a higher-resolution mosaic of a specific region, it is possible to create a multispectral mosaic, starting from raw or calibrated data available on ODE Mercury. Mercury MDIS-WAC data can be easily reduced by using the ISIS3.5.2 (https://isis.astrogeology.usgs.gov/Application/index.html) and following the MESSENGER MDIS tutorial available in the Planetary Data System (PDS) website (https://pds-imaging.jpl.nasa.gov/documentation/MESSENGER_MDIS_WorkShop_LPSC2103.pdf).

The steps to create the 8-color reflectance mosaic are the following:

2. Select the EDR (Experiment Data Record) images of the region of interest from ODE-Mercury.
3. Calibrated the EDR images taking into account the calibration available in ISIS3.5.2 software and including: 1- dark current correction; 2- linearity correction; 3- readout smear correction; 4- uniformity (flat field) correction; 5- absolute coefficient correction; 6- conversion to irradiance over solar flux (I/F); empirical correction (see Denevi et al., 2018).
4. Applied the Kaasalainen-Shkuratov photometric correction model considering the parameters derived by Domingue et al. 2016. The images were normalized to standard photometric geometries of 30° incidence angle, 0° emission angle and 30° phase angle. To apply the topography correction, the user can consider the Digital Elevation Model (DEM) provided by the Deutsches Zentrum fur Luft und Raumfahrt (DLR) with a spatial resolution of 222 m/pixel (Preusker et al. 2017). This is the best DEM currently available, and it has been produced for only a few Mercury quadrangles (https://pds-imaging.jpl.nasa.gov/data/messenger/messdem_1001/DEM/QUAD/IMG/). The application of this DEM is essential to accurately correct the local topographic effects in the high spatial resolution images. Alternatively, the Mercury MESSENGER Global DEM at 665 m/pixels can be considered (https://astrogeology.usgs.gov/search/map/Mercury/Topography/MESSENGER/Mercury_Messenger_USGS_DEM_Global_665m_v2).

5. Project the photometrically corrected images using the best projection required for your specific case.
6. Coregister the images of each 8-filter set with respect to one of the filters.
7. Created the 8-filter cubes ordered by increasing wavelengths. The quadrangle mosaic is constructed with the mean value of the overlapping pixels for each filter.

The **MASCS** instrument Cassegrain telescope simultaneously feeds light to both a VIRS spectrometer and an UVVS. VIRS, a point spectrometer with a 0.023° field of view and two linear array detectors, has two channels: one covering the visible (VIS) from 300 nm to 900 nm and a near-infrared detector (NIR) covering 900 nm to 1450 nm, both at a spectral resolution of 5 nm (McClintock and Lankton, 2007; Holsclaw et al. 2010; Izenberg et al. 2014) for 494 combined wavelengths. The instrument operational temperature varies based on orbital and seasonal changes in thermal load from Mercury (Izenberg et al. 2014). The NIR detector displays increased background and noise from elevated temperatures compared to the VIR detector, and thus also displays 3 – 5 times lower signal-to-noise ratios (SNRs) than the VIS detector (Izenberg et al. 2014). A more detailed description of the instrument calibration can be found in Holsclaw et al. (2010) and Izenberg et al. (2014).
In particular, VIRS-VIS have been used to produce Mercury multispectral global maps in the Visible-Near Infrared.
An example of those data for the single wavelength 750 nm are at MESSENGER QuickMap (https://messenger.quickmap.io) and available at the NASA/PDS Geosciences Node Data and Services for MESSENGER/MASCS (https://pds-geosciences.wustl.edu/missions/messenger/mascs.htm) or from ODE. Those products do not include the latest photometric correction, but a previous empirical attempt to compensate for the photometric effect.
More complete VIRS-VIS Mercury multispectral global maps covering the whole detector range and interpolated to a fixed grid have been produced as part of the ML work package and will be available through the VESPA infrastructure.
The code and workflow is available as a python jupyter notebook on the github public repository on github.com/epn-ml public repository.

2.4 Vesta

The NASA/Dawn mission collected imagery, topography and hyperspectral global data from Vesta. Scientific results from the analysis of Dawn VIRs data (De Sanctis et al. 2011) confirmed that the Vesta surface is compositionally diverse (e.g. Ammannito et al., 2013). Dawn's data from Vesta is available from the PDS nodes in the form of raw and processed data.

3. Preliminary spectral analysis (spectral indices)

In general, the first approach for a spectral data analysis is to understand the spectral variation and try to emphasize the absorptions, reflectance and slope differences. To do these three main spectral indices have to be taken into account:

Typical Band Centre: Band centres are sensitive to compositional variations within minerals. It is in general calculated after the continuum removal to avoid effects of slope variation due to other physical properties or the presence of phases with a featureless but with a strong slope. In order to remove the continuum, we have properly selected the absorption band and we calculated the maximum of the two shoulders of the band. We then calculated the straight line (or in some cases if polynomial continuum could be considered, even if less common) passing between the two shoulders (continuous). Then we divided the selected band by the straight line of the continuum. After the continuum removal, we identified a neighbourhood of the band minimum. If the minimum region is narrow we could even select the absolute minimum or if absorption is quite broad (or instrumental artefact could be present in the same spectral range), we approximated the band minimum neighbourhood by fitting it with a II degree polynomial. Therefore, we have been able to calculate the wavelength corresponding to the minimum of this polynomial, which is exactly the band centre (e.g. see also Clark and Roush 1984, Cloutis et al 1989, Clark 1999, Ammannito et al. 2013).

Typical Band Depth: Following Clark and Roush (1984), the band depths are defined as: 1-Rb/Rc where Rb is the reflectance at the band minimum and Rc is the reflectance of the spectral continuum at the same wavelength.

Typical Spectral Slope: The spectral slopes were calculated using the same definition of Cuzzi et al. (2009), Filacchione et al. (2012), see also PLANMAP deliverable 4.1, 4.2 and 4.3. (https://wiki.planmap.eu/display/public/Deliverables).

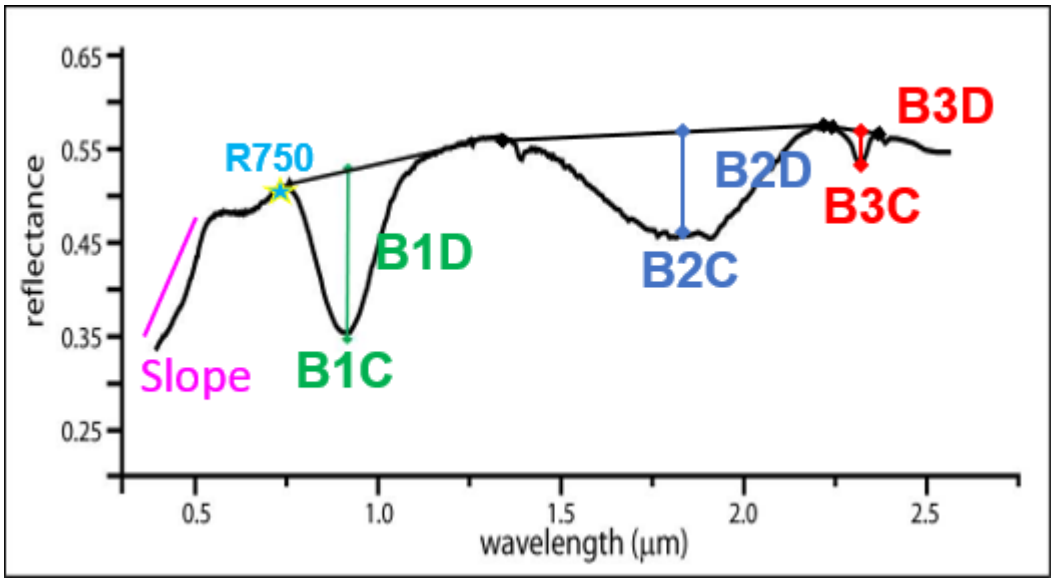

Figure 1: example of spectral indices: reflectance at 0.75 μm; BnC, the band centres in different positions; BnD, the band depth for the different bands; and an example of spectral slope.

3.1. The Moon

For the Lunar case, the main absorption bands observed are those centred at 1 and 2 μm associated with the presence of pyroxenes. Laboratory studies indicate that band centres are shifted towards longer wavelengths for increasing Fe^{2+} abundance (Gaffey, 1976; Klima et al., 2007, 2011). Similar shifts could be associated also to a variation in abundance of mineralogical phases within rocks like variable abundances of olivine, spinel, plagioclase (where abundant) or glasses. All these phases affect mainly the 1 μm, only chromite can influence the 2 μm band. Band depths can be related to the abundance of the primary absorbing minerals, so on the Moon often different ratios among pyroxenes with respect to olivine, plagioclase, and/or the abundance of opaque materials. Even regions with similar absorptions but different reflectance and band depths could indicate different particle size.

The Lunar surface is characterized by a red spectral slope due to the production of nFe0 particles caused by space weathering effects (Pieters and Noble, 2016). The analysis of this parameter is important to correlate the terrain maturity, compositional and grain size variations, with space weathering processes.

3.2 Mars

Martian spectral parameters are slightly different between the OMEGA and CRISM dataset, to take into account the different specifics of the two instruments.

For the OMEGA dataset, the spectral parameters for key surface materials detections, i.e. mafic iron-bearing silicates, hydrated minerals, ferric oxides, and ices are listed and described in detail in Poulet et al. (2007). These parameters were adapted by Ody et al. (2012) to take into account the aging of the C-channel detector and the new calibration procedure of the visible channel and used for preparation of global maps of anhydrous minerals. They are also used in global-scale study of hydrated minerals presented in Carter et al. (2013), which is an example of integrated OMEGA and CRISM analysis. Specific parameters for the 1 μm band, attributable to iron in various materials can be also found in Carrozzo et al. (2012).

The investigation of CRISM hyperspectral data can be carried out using several spectral parameters which are designed to highlight a great variety of spectral signatures which could be present in the dataset. One of the most commonly used parameters is the band depth. Sometimes the absorption feature can be a doublet, or it can be very broad, spanning many wavelengths sampled by CRISM. In these cases, the band depth parameters are combined into other types of parameters to characterize the feature of interest. The definition of all the spectral parameters which can be used with CRISM data is provided by the CRISM team in Viviano-Beck et al (2014). In total, 60 parameters are available to characterize the surface mineralogy of Mars. Previous

work that converted OMEGA's spectral parameters into CRISM spectral parameters is described by Pelkley et al. (2007).

3.3 Mercury

Mercury surface is characterized by the lack of absorption bearing features at the spatial resolution of MDIS-WAC data, except for few cases, e.g. hollows regions.
Hollows are small depressions formed where volatiles have been lost from the surface (e.g. Blewett et al., 2011, 2013, 2016; Thomas et al., 2016). Hollows have peculiar spectral characteristics, in some cases, e.g. Dominici crater, they show an absorption band at 600 nm (Vilas et al., 2016; Lucchetti et al., 2018).
The surface of mercury surface shows a widespread distribution of low reflectance material, due to the presence of C in the form of graphite, is the most suitable opaque phase for Mercury (e.g. Murchie et al. 2015; Klima et al. 2018). The percentage of graphite is estimated ~ 1 wt%, while in low reflectance material it can reach ~ 5 wt% (Murchie et al., 2015; Klima et al., 2018). The LRM have been interpreted as a typical example of the exposure of Mercury graphite-rich floating crust, surviving impacts and volcanism.
Klima et al. (2018) studied the global distribution of low reflectance material. They observed the 600-nm band depth in LRM is linked to carbon content and can be used to estimate carbon enrichment.
In this case, spectral slope together with reflectance is the main spectral parameter which better helps to discriminate the spectral variation of the Hermean surface (see Zambon et al. (2021, in press), and PLANMAP Deliverables 4.2 and 4.3 (https://wiki.planmap.eu/display/public/Deliverables)).
Attempts to extract and classify surfaces based on spectra spectral characteristics have been described in D'Amore et al (2021) on the basis of global MASCS gridded data. These are available through the EPN DLR Machine Learning WP and in VESPA.
Barraud et al. (2021) constraints on the planet's explosive activity investigating Mercury's pits' surroundings and the dimensions of the faculae, geomorphological structure peculiar to Mercury.

3.4 Vesta

Vesta reflectance spectra clearly show that the surface is variegated even if the spectra are always and strongly characterized by two specific absorptions around 1 and 2 µm (e.g. De Sanctis et al. 2012a) attributable to pyroxenes (Burns 1993). The range of variability of these absorptions are compatible with the HEDs as already suggested (e.g. Beck et al. 2013; Burbine et al. 2001). These parameters have been studied considering the position variation and their band depth variation. Potential presence of olivine has been suggested due to the spectral variability of the 1µm absorption (e.g. Ammannito et al. 2013; Ruesh et al. 2014; Poulet et al. 2015; Palomba et al 2015). Additionally hydration has been investigated due to the presence of a band at 2.8 µm (De Sanctis et al. 2012b).

4. High level product (Spectral indices maps, RGB, Colour mosaics)

In this section we recall where for the bodies and datasets introduced before we can find high level products that can be helpful for mapping, to superimpose already information related to the composition on maps produced considering other geological information.

4.1 Moon

Starting from a calibrated and photometrically corrected hyperspectral image cube of mosaic, the user can produce all the high-level products necessary for the spectral analysis.

As mentioned above, for the Moon case the main spectral indices map are those of the band centres and depths of the two pyroxenes bands at 1 and 2 µm and spectral slopes. In addition to these spectral indices, specific RGB images can be worthwhile to identify spectral variations. Apart from the potential global data from the M^3 spectral images, for the Moon are available, with helpful retrieved composition also data from the Clementine results, that here we also indicate, since they could be helpful to compositionally study the different characteristics of the Moon surface.

Clementine RGB colour composite mosaic, is the main RGB colour combination considered for the Moon. Red channel represents areas characterized by low titanium or high glass content (redder spectral slope), the green channel is sensitive to the amount of iron (band centre shifted toward longer wavelengths, and deeper band depth), and the blue channel reflects the surfaces with high titanium or materials with bright slopes and albedos that are not compensated by using the image ratios (bluer spectral slope). Lunar highlands appear red in clementine RGB colour combination because they have accumulated glassy agglutinates produced during the bombardment of micrometeorites (maturation) (red spectral slope). Red in the false-colour image are also pyroclastic deposits because of their high-glass content. The yellow-green areas within the mare is the combined effect of concentration of mafic minerals (green) and the glass in the soil produced by maturation (red). The blue units are typical of the Moon maria and smooth plains and correspond relatively higher in titanium compared to the mare unit immediately to the north.

Global Clementine maps of the Moon are available at the following links:
https://astrogeology.usgs.gov/search/map/Moon/Clementine/UVVIS/Lunar_Clementine_UVVIS_Warp_ClrRatio_Global_200m,
https://astrogeology.usgs.gov/search/map/Moon/Clementine/UVVIS/Lunar_Clementine_UVVIS_750nm_Global_Mosaic_118m_v2,
https://astrogeology.usgs.gov/search/map/Moon/Clementine/UVVIS/Lunar_Clementine_UVVIS_FeO_ClrBinned_70S70N_1km,
https://astrogeology.usgs.gov/search/map/Moon/Clementine/UVVIS/Lunar_Clementine_UVVIS_WarpMosaic_5Bands_200m.

Spectral parameters and spectral units maps of Apollo, Von Karman and Leibnitz regions are shown in PLANMAP deliverable D4.3 and D4.4, are available on Zenodo at the following links:
https://doi.org/10.5281/zenodo.4772473,
https://doi.org/10.5281/zenodo.4772495,
https://doi.org/10.5281/zenodo.4772355.
Other RGB colour combinations are also useful to discriminate spectral variabilities, e.g. R: spectral slopes calculated between the shoulder of the 1 µm band, G: band depth at 1 µm, B: band depth at 2 µm. This RGB combination is representative of the space weathering effects on the Moon spectra. Higher values of the 1 µm band spectral slope and low values of BDI and BDII could represent regions where space weathering effects are more efficient (see PLANMAP 4.3 deliverable (https://wiki.planmap.eu/display/public/Deliverables) and Zambon et al. in preparation).

4.2 Mars

ESA PSA Global Maps of Mars (https://www.cosmos.esa.int/web/psa/mars-maps) provides quick access to the maps derived from the reflectance data acquired by the Mars Express OMEGA hyperspectral camera. Currently available are: the NIR 1-micrometer albedo map, and the pyroxene (Figure 2), olivine and ferric oxide spectral parameter maps by Ody et al. (2012), and a map of hydrated mineral sites by Carter et al. (2013). The OMEGA Mars Global Maps data set can also be browsed and visualised in Google Earth.

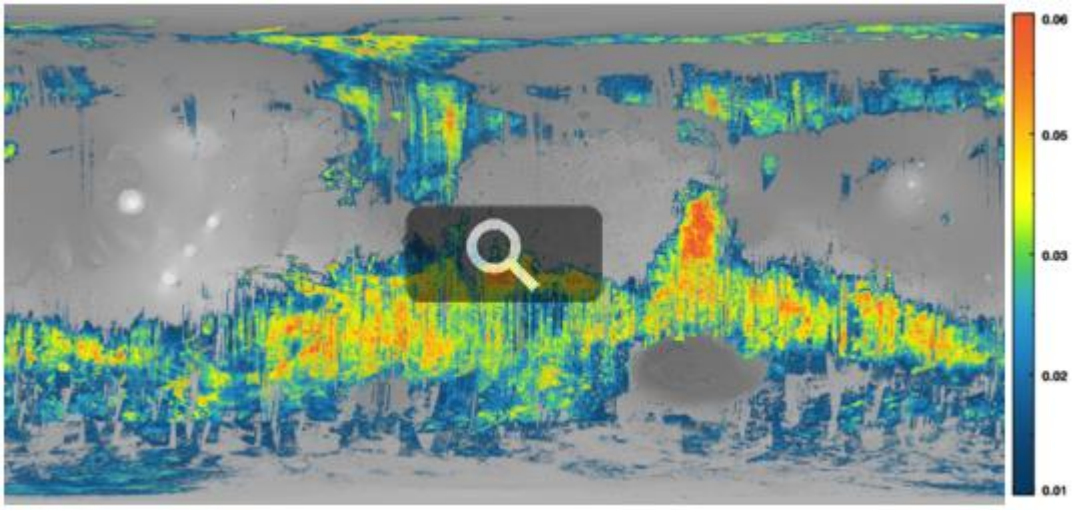

Figure 2: Example of data product in ESA PSA Global Maps of Mars: Global pyroxene spectral parameter map of Mars based on reflectance data acquired by the Mars Express OMEGA hyperspectral camera from January 2004 to August 2010. The pyroxene spectral parameter (BD2000) is based on its 2 µm absorption band due to both high-calcium and low-calcium pyroxene (Ody et al., 2012). Products to download: PDS Label, PDS Image, ISIS Cube, GeoTIFF.

The MICA Files, available at this link http://crism.jhuapl.edu/data/mica/, contains an overview of key mineral deposits on Mars. For each mineral, a two-page standardized

set of information is provided, including for example type locations, spectral properties of the mineral and a RGB map of spectral products. CRISM spectra presented in the MICA files can also be downloaded here: https://crismtypespectra.rsl.wustl.edu along with similar laboratory spectra. RGB maps of CRISM spectral parameters (browse products) are downloadable from ODE/PDS archive (https://ode.rsl.wustl.edu/mars/). In figure 3 there is an example of the map tool available to browse CRISM files. Once a file is selected (figure YYYb), RGB maps can be downloaded in the "browse files" section in the "PDS Product Files" menu. Figure 3 lists some examples of CRISM RGB maps downloaded from ODE.

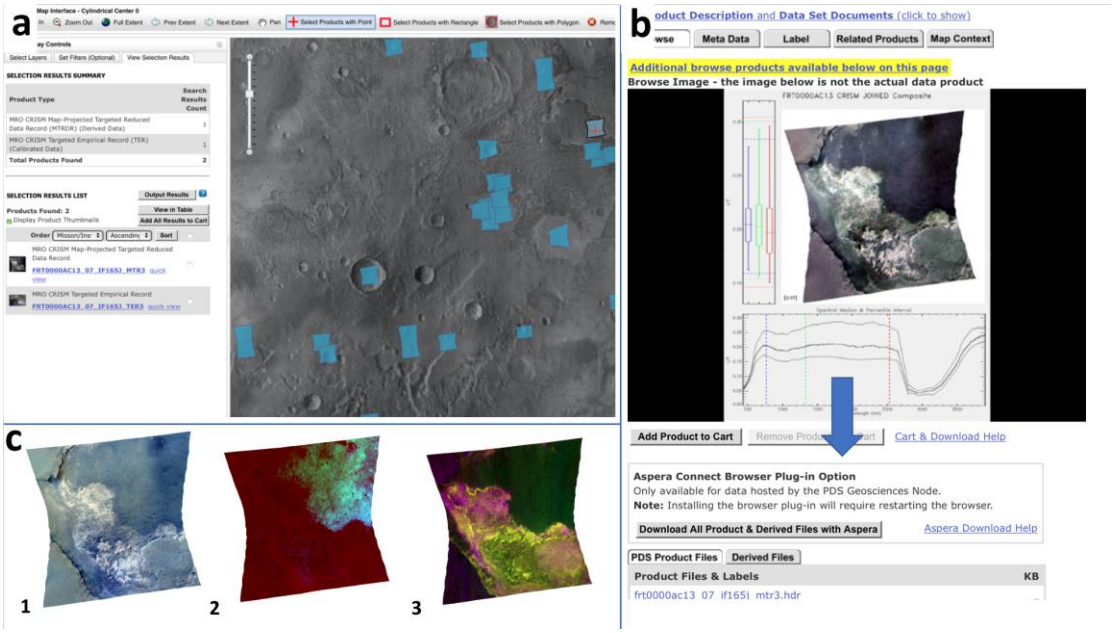

Figure 3: (a) Example of CRISM product search via ODE/PDS, CRISM footprints in the chosen area are here shown in blue. (b) The RGB maps are available to download in the product page, under the "browse files" section, which can be found scrolling down in the "PDS Product Files" menu. (c) Example of RGB maps: true color visible RGB map (c1), mafic mineralogy (c2), and hydrated mineralogy (c3).

4.3 Mercury

To retrieve the MDIS-WAC high level products, it is necessary the multispectral colour mosaic. The user can download the MESSENGER/MDIS-WAC global 8-color mosaic at 665 m/pixel at the following link: https://messenger.jhuapl.edu/Explore/Images.html#global-mosaics, or produce by him/herself the multispectral mosaic of a specific area as indicated in section *"Mercury MESSENGER/MDIS-WAC dataset"* of this document.

Mercury basemaps and high level products are available at the following links: https://astrogeology.usgs.gov/search/map/Mercury/Messenger/Global/Mercury_MESSENGER_MDIS_Basemap_LOI_Mosaic_Global_166m, https://astrogeology.usgs.gov/search/map/Mercury/Messenger/Global/Mercury_MESSENGER_MDIS_Basemap_EnhancedColor_Mosaic_Global_665m,

https://astrogeology.usgs.gov/search/map/Mercury/Messenger/Global/Mercury_MESSENGER_MDIS_Basemap_MD3Color_Mosaic_Global_665m,
https://astrogeology.usgs.gov/search/map/Mercury/Messenger/Global/Mercury_MESSENGER_MDIS_Basemap_BDR_Mosaic_Global_166m,
https://astrogeology.usgs.gov/search/map/Mercury/Messenger/Global/Mercury_MESSENGER_MDIS_Basemap_LOI_Mosaic_Global_166m,
https://astrogeology.usgs.gov/search/map/Mercury/Messenger/Global/Mercury_MESSENGER_MDIS_ClrMosaic_global_665m_v3,
https://astrogeology.usgs.gov/search/map/Mercury/Topography/MESSENGER/Mercury_Messenger_USGS_ClrShade_Global_2km,
https://astrogeology.usgs.gov/search/map/Mercury/Topography/MESSENGER/Mercury_Messenger_USGS_DEM_Global_665m_v2,
https://messenger.jhuapl.edu/Explore/Images.html#global-mosaics.
Several examples of Mercury high level products are reported in Zambon et al. 2021 in press, and in PLANMAP D4.2, 4.3, 4.4 deliverables (https://wiki.planmap.eu/display/public/Deliverables). Spectral indices maps of H05-Hokusai quadrangle (https://doi.org/10.5281/zenodo.4772509, https://doi.org/10.5281/zenodo.4772274), Beethoven (https://doi.org/10.5281/zenodo.4772419) and Rembrandt (https://doi.org/10.5281/zenodo.4772459) basins are available on Zenodo.
For MASCS data, high level products will be released in the near future, up to now material as code and workflow is available as a python jupyter notebook on the github public repository on github.com/epn-ml public repository.

4.4 Vesta

Another interesting case where it is possible to find high level products is the surface of Vesta. The VIR team in fact released the maps for each global mosaic GIS-ready spectral indices from the VIR VIS/IR spectrometers that have been published by INAF/IAPS (doi:10.7910/DVN/JJJL6R). An example for the Band Centre at 2m is reported in figure 4**.**
The variety of different terrains on Vesta led to the compilation of a geologic map (figure 5). This digital map data have not been published yet, but Volume 244 of Icarus published in 2014 groups all the mapping efforts of the quadrangle-based geologic mapping of Vesta.

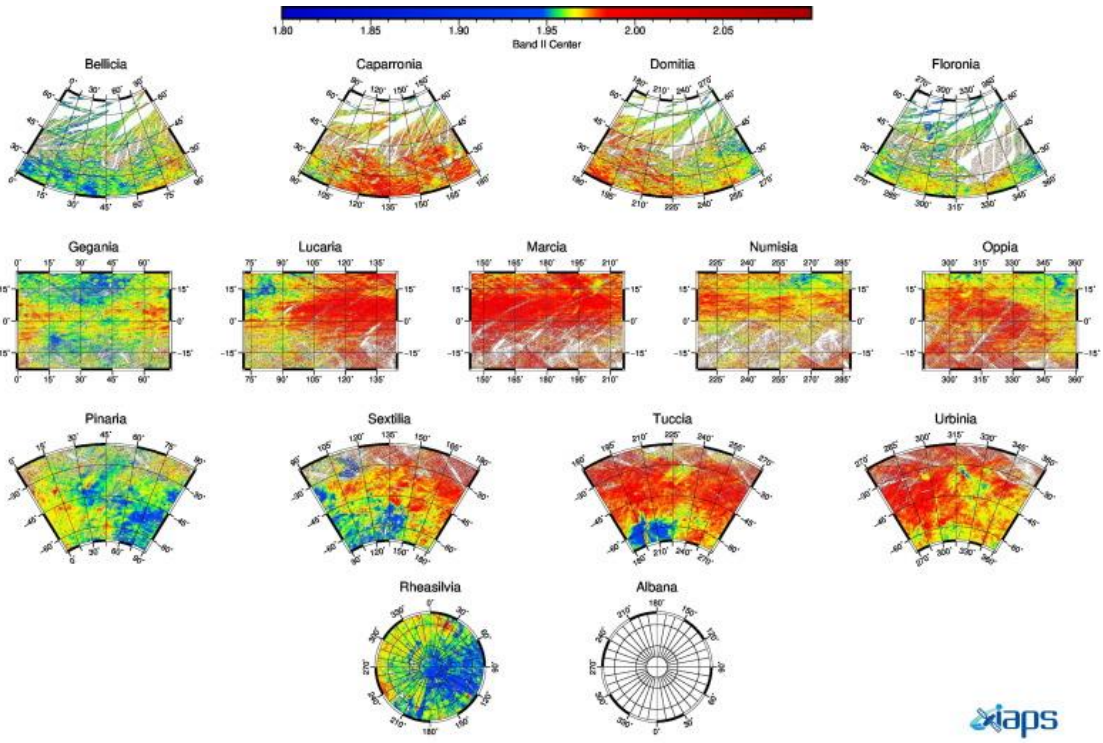

Figure 4: Quadrangle maps released for the different Band Centers and depths calculated from VIR, here and examples from the Band Center 2. The quadrangle can be downloaded by the link.

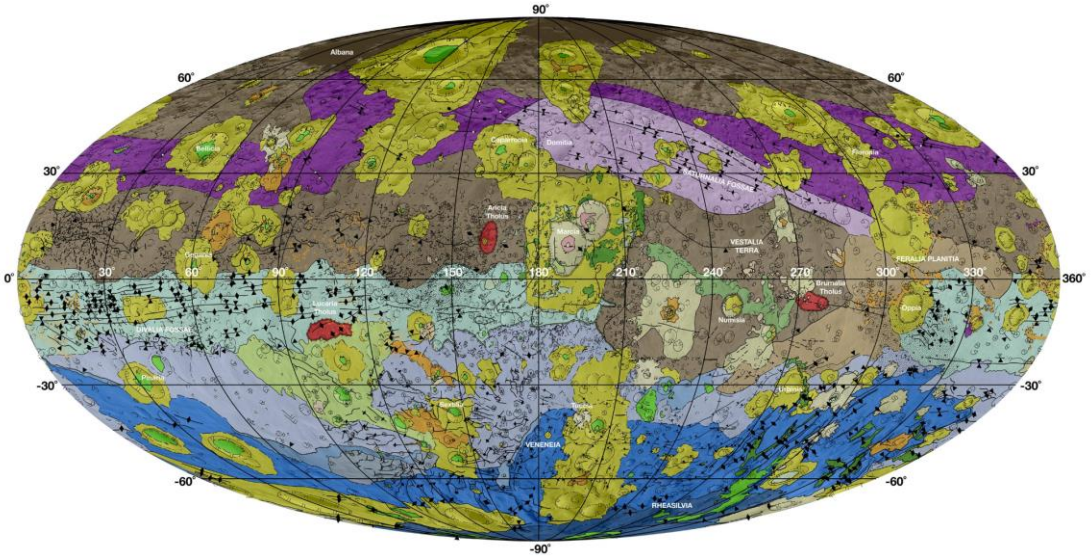

Figure 5. The geologic map of Vesta. No digital map has been published yet, Icarus volume 144 collects articles about quadrangle-mapping efforts.

REFERENCES:

Ammannito E. et al. 2013. Vestan lithologies mapped by the visual and infrared spectrometer on Dawn. M&PS. 48, 2185-2198.

Beck, A.W., et al. 2013. Challenges in detecting olivine on the surface of 4 Vesta. Meteorit. Planet. Sci. 48, 2155–2165.

Barraud, O., et al.. 2021. Spectral investigation of Mercury's pits' surroundings: Constraints on the planet's explosive activity. Icarus, 114652. https://doi.org/10/gmhh6p

Bishop, J.L., Bell III, J.F., and , Moersch, J.E. 2019. Remote Compositional Analysis. Cambridge University Press. https://doi.org/10.1017/9781316888872.

Blewett, D. T., et al. 2011. Hollows on Mercury: MESSENGER Evidence for Geologically Recent Volatile-Related Activity.Science, 333,1856. doi: 10.1126/science.1211681

Blewett, D. T., et al. 2016. Analysis of MESSENGERhigh-resolution images of Mercury's hollows and implications for hollow formation. Journal of Geophysical Research (Planets), 121, 1798-1813.doi:10.1002/2016JE005070

Blewett, D. T., et al., 2013. Mercury's hollows: Constraints on formation and composition from analysis of geological setting and spectral reflectance.Journal of Geophysical Research (Planets), 118, 1013-1032.doi:10.1029/2012JE004174.

Burbine, T.H., et al. 2001. Vesta, Vestoids, and the HEDs: relationships and the origin of spectral differences. Meteorit. Planet. Sci. 36 (6), 761–781. https://doi. org/10.1111/j.1945-5100.2001.tb01915.x.

Burns, R. 1993. Mineralogical Applications of Crystal Field Theory. Second Edition. Cambridge University Press

Carrozzo, F. G. et al. 2012. Iron mineralogy of the surface of Mars from the 1 μm band spectral properties, J. Geophys. Res. Planets 117, E00J17, doi:10.1029/2012JE004091.

Carter, J., et al. 2013. Hydrous minerals on Mars as seen by the CRISM and OMEGA imaging spectrometers: Updated global view, J. Geophys. Res. Planets 118, doi:10.1029/2012JE004145.

Christensen, P.R., et al. 1992. Thermal emission spectrometer experiment: Mars Observer Mission. JGR 97, 7719-7734.

Christensen, P.R., et al. 2004. The Thermal Emission Imaging System (THEMIS) for the Mars 2001 Odyssey Mission. Space Science Reviews, v. 110, Issue 1, 85-130.

Clark R. and Roush T. L. 1984. Reflectance spectroscopy: Quantitative analysis techniques for remote sensing applications. J. Geophys. Res. doi:10.1029/JB089iB07p06329.

Clark, R. N., et al. 1990. High spectral resolution reflectance spectroscopy of minerals. Journal of Geophysical Research, 95, 12653–12680. DOI: 10.1029/JB095iB08p12653.

Clark, R.N. , 1999, vol. 3. Remote Sensing for the Earth Sciences—Manual of Remote Sensing. John Wiley and Sons, New York .

Cloutis E. 1989. Calibrations of phase abundance, composition, and particle size distribution for olivine-orthopyroxene mixtures from reflectance spectra. 91, 11641-11653.

Cuzzi, J., et al. 2009. Ring Particle Composition and Size Distribution.InM. K. Dougherty, L. W. Esposito, & S. M. Krimigis (Eds.),Saturn fromcassini-huygens (p. 459). DOI: 10.1007/978−1−4020−9217−615.

D'Amore, M., et al., 2021, Unsupervised classification of Mercury'S Visible-Near-Infrared MASCS/MESSENGER reflectance spectra for automated surface mapping., EGU21-2661, EGU General Assembly Conference Abstracts, 2021EGUGA..23.2661D.

De Sanctis, M.C., et al. 2011. The VIR spectrometer. Space Sci. Rev. 163, 329–369. https://doi.org/10.1007/s11214-010-9668-5.

De Sanctis, M.C., et al. 2012a. Spectroscopic characterization of mineralogy and its diversity across Vesta. Science 336, 697–700. https://doi.org/10.1126/science.1219270.

De Sanctis, M.C., et al. 2012b. Detection of widespread hydrated materials on Vesta by the VIR imaging spectrometer on board the DAWN mission. The Astrophysical Journal Letters, 758:L36. doi:v10.1088/2041-8205/758/2/L36

Domingue, D.L., et al. 2014. Mercury's Weather-Beaten Surface: Understanding Mercury in the Context of Lunar and Asteroidal Space Weathering Studies. Space Sci Rev 181, 121–214 (2014). https://doi.org/10.1007/s11214-014-0039-5

Farmer, V.C., 1974. The Infrared Spectra of Minerals. Mineralogical Society of Great Britain and Ireland.

Filacchione, G., et al. 2012. Saturn's icy satellites and rings investigated by Cassini–VIMS: III – Radial compositional variability.Icarus,320, 1064-1096.DOI: 10.1016/j.icarus.2012.06.040.

Gaffey, M. J., 1976. Spectral reflectance characteristics of the mete-orite classes.Journal of Geophysical Research,81, 905-920. DOI:10.1029/JB081i005p00905.

Hawkins, S. E., et al. 2007. The Mercury Dual Imaging System on the MESSENGER Spacecraft. Space Science Reviews, 131(1-4), 247-338. doi:10.1007/s11214-007-9266-3

Holsclaw, G. M., et al. 2010, A comparison of the ultraviolet to near-infrared spectral properties of Mercury and the Moon as observed by MESSENGER, *Icarus*, *209*(1), 179-194, DOI:10.1016/j.icarus.2010.05.001

Izenberg, N. R., et al. 2014, The low-iron, reduced surface of Mercury as seen in spectral reflectance by MESSENGER, 228, 364-374, Icarus, DOI:10.1016/j.icarus.2013.10.023

Klima, R.L., et al., 2007. Spectroscopy of synthetic Mg-Fe pyroxenes I: Spin-allowed and spin-forbidden crystal field bands in the visible and near-infrared. Meteorit. Planet. Sci. 42, 235–253.

Klima, R. L., et al. 2011. Near-infrared spectra of clinopyroxenes: Effects of calcium content and crystal structure. Meteoritics&Planetary Science,46, 379-395. DOI: 10.1111/j.1945-5100.2010.01158.x.

Klima, R. L., Denevi, B. W., Ernst, C. M., Murchie, S. L., & Peplowski, P. N.(2018).Global distribution and spectral proper- ties of low-reflectance mate-rial on Mercury.Geophysical Research Letters,45 (2945–2953). Doi: 10.1002/2018GL077544

Lucchetti A., et al. 2018. Mercury Hollows as Remnants of Orig-inal Bedrock Materials and Devolatilization Processes: A Spectral Clusteringand Geomorphological Analysis.Journal of Geophysical Research (Planets),123(9), 2365-2379. DOI: 10.1029/2018JE005722

McClintock, W. E., Lankton, M. R. , 2007, The Mercury Atmospheric and Surface Composition Spectrometer for the MESSENGER Mission, 131, 481-521, Space Science Reviews, DOI:10.1007/s11214-007-9264-5

McGuire, P. C., et al., 2009. An improvement to the volcano-scan algorithm for atmospheric correction of CRISM and OMEGA spectral data. Planetary and Space Science, 57, 809-815. DOI: 10.1016/j.pss.2009.03.007.

McEwen, A. S., & Robinson, M. S. 1997. Mapping of the Moon by Clementine. Advances in Space Research, 19(10), 1523-1533. https://doi.org/10.1016/S0273-1177(97)00365-7

Murchie, S. L., et al., 2007. Compact Reconnaissance Imaging Spectrometer for Mars (CRISM) on Mars Reconnaissance Orbiter (MRO). Journal of Geophysical Research (Planets), 112 (E5). DOI: 10.1029/2006JE002682

Murchie, S. L., et al., 2015. Orbital multispectral mapping of Mercury with the MESSENGER Mercury Dual Imaging System: Evidence for the origins of plains units and low-reflectance material. Icarus,254, 287-305. doi:95810.1016/j.icarus.2015.03.027

Ody, A., et al. 2012. Global maps of anhydrous minerals at the surface of Mars from OMEGA/MEx, J. Geophys. Res. Planets 118, doi:10.1029/2012JE004117.

Paige, D.A., et al. 2010. The Lunar Reconnaissance Orbiter Diviner Lunar Radiometer Experiment. Space Science Reviews 150, 125-160.

Pelkey, S. M., et al. 2007, CRISM multispectral summary products: Parameterizing mineral diversity on Mars from reflectance, J. Geophys. Res., 112, E08S14, doi:10.1029/2006JE002831

Pieters C. M. et al. 2009. The Moon Mineralogy Mapper (M 3) on Chandrayaan-1. CURRENT SCIENCE. 96, 4.

Pieters, C. M., & Noble, S. K. 2016.Space weathering on airless bod-ies.Journal of Geophysical Research (Planets),121(10), 1865-1884. DOI:10.1002/2016JE005128.

Palomba, E., et al. , 2015. Detection of new olivine- rich locations on Vesta. Icarus 258, 120–134 .

Poulet, F., et al. 2007. Martian surface mineralogy from Observatoire pour la Minéralogie, l'Eau, les Glaces et l'Activité on board the Mars Express spacecraft (OMEGA/MEx): Global mineral maps, J. Geophys. Res. Planets 112, E08S02, doi:10.1029/2006JE002840.

Poulet, F., et al. 2018. PSUP: A Planetary SUrface Portal, Planet. Space Sci. 150, 2-8, doi:10.1016/j.pss.2017.01.016.

Poulet, F., et al. 2015. Modal mineralogy of the surface of Vesta: Evidence for ubiquitous olivine and identification of meteorite analogue. Icarus 253, 354–377 .

Quantin-Nataf, C., et al. 2018. MarsSI: Martian surface data processing information system, Planet. Space Sci. 150, 157-170, doi:10.1016/j.pss.2017.09.014

Richards, J. A. Remote Sensing Digital Image Analysis: An Introduction, Springer-Verlag, 1999.

Rothery, D., et al. 2020. Rationale for BepiColombo studies of Mercury's surface and composition. Space Sci. Rev. 216 (4), 66. https://doi.org/10.1007/s11214-020-00694-7.

Ruesch, O., et al. 2014. Detections and geologic context of local enrichments in olivine on Vesta with VIR/Dawn data. J. Geophys. Res. Planets 119, 2078–2108. https://doi.org/10.1002/2014JE004625.

Thomas, R., et al. 2016. Mercury's low-reflectance material: Constraints from hollows. Icarus, 277, 455-465. Doi: 10.1016/j.icarus.2016.05.036.

Vilas, F., et al. 2016. Mineralogical indicators of Mercury's hol-lows composition in MESSENGER color observations. Geophysical Research Letters,43(4), 1450-1456. DOI: 10.1002/2015GL067515

Viviano-Beck, C. E., et al., 2014. Revised CRISM spectral parameters and summary products based on the currently detected mineral diversity on Mars. Journal of Geophysical Research (Planets), 119 (6), 1403–1431. DOI: 10.1002/2014JE004627.

Zambon F., et al. 2021, Spectral units analysis of quadrangle H05-Hokusai on Mercury, Journal of Geophysical Research (Planets), in press.